

# The Journal of Clinical Pharmacology

<http://www.jclinpharm.org>

---

## Population Pharmacokinetics of Mycophenolic Acid and Its 2 Glucuronidated Metabolites in Kidney Transplant Recipients

Wai-Johnn Sam, Fatemeh Akhlaghi and Sara E. Rosenbaum  
*J. Clin. Pharmacol.* 2009; 49; 185  
DOI: 10.1177/0091270008329558

The online version of this article can be found at:  
<http://www.jclinpharm.org/cgi/content/abstract/49/2/185>

---

Published by:



<http://www.sagepublications.com>

On behalf of:

American College of Clinical Pharmacology

Additional services and information for *The Journal of Clinical Pharmacology* can be found at:

**Email Alerts:** <http://www.jclinpharm.org/cgi/alerts>

**Subscriptions:** <http://www.jclinpharm.org/subscriptions>

**Reprints:** <http://www.sagepub.com/journalsReprints.nav>

**Permissions:** <http://www.sagepub.com/journalsPermissions.nav>

---

# Population Pharmacokinetics of Mycophenolic Acid and Its 2 Glucuronidated Metabolites in Kidney Transplant Recipients

Wai-Johnn Sam, PhD, Fatemeh Akhlaghi, PhD, and Sara E. Rosenbaum, PhD

---

The population pharmacokinetics of mycophenolic acid (MPA) and its phenolic (MPAG) and acyl (AcMPAG) glucuronide metabolites were studied in patients taking enteric-coated mycophenolate sodium. Plasma samples ( $n = 232$ ), obtained from 18 renal transplant recipients, were analyzed for MPA, MPAG, and AcMPAG using a validated high-performance liquid chromatography/ultraviolet assay. Population pharmacokinetic analysis was performed using NONMEM. The pharmacokinetics of MPA were best described by a 2-compartment model, with MPAG and AcMPAG produced from the central compartment and with enterohepatic recirculation of MPA via these 2 metabolites. Population mean estimates for MPA were apparent clearance ( $CL/F$ ) of 10.6 L/h (interindividual variability [IIV] = 21.4%) and apparent volume of distribution of the central compartment ( $V_1/F$ ) of 25.9 L (IIV = 87.8%). Mean elimination rate constants of MPAG and

AcMPAG were  $0.323 \text{ h}^{-1}$  (IIV = 29.1%) and  $0.206 \text{ h}^{-1}$  (IIV = 48.8%), respectively. The mean fraction of MPA converted to MPAG and AcMPAG, normalized by their volumes of distribution ( $FM_{AG}$  and  $FM_{AC}$ , respectively), was also estimated. The elimination rate constant for MPAG and  $FM_{AC}$  was influenced by glomerular filtration rate in patients with renal impairment. The visual predictive check, based on 100 simulated data sets each for MPA, MPAG, and AcMPAG, found that the final pharmacokinetic model adequately predicts the observed concentrations of all 3 species.

**Keywords:** acyl MPAG; enterohepatic recirculation; GFR; renal transplant; MPAG; mycophenolic acid; NONMEM; population pharmacokinetics

*Journal of Clinical Pharmacology*, 2009;49:185-195  
© 2009 the American College of Clinical Pharmacology

---

Mycophenolic acid (MPA) is a noncompetitive, selective, and reversible inhibitor of inosine monophosphate dehydrogenase (IMPDH), a rate-limiting enzyme involved in the purine synthesis pathway. This leads to inhibition of the de novo synthesis of guanosine nucleotides in lymphocytes, followed by arrest of the proliferation and function of these cells.<sup>1</sup> Following solid organ transplantation, MPA is used in combination with calcineurin inhibitors, cyclosporine or tacrolimus, and prednisone to prevent acute allograft rejection. Even though MPA is

generally well tolerated, adverse effects, including infections, leucopenia, and gastrointestinal disturbances, are associated with its use. An enteric-coated formulation of mycophenolate sodium has been developed to help reduce the gastrointestinal side effects of MPA.

Mycophenolic acid is about 95% bound to plasma proteins, including albumin.<sup>2</sup> It is metabolized by hepatic and renal UDP glucuronosyltransferases (UGTs) at the phenolic hydroxyl group to form a 7-O-glucuronide conjugate (MPAG), which is pharmacologically inactive.<sup>3</sup> Although MPAG may not directly contribute to immunosuppression, it competes with MPA at the plasma protein binding level and may increase the free and pharmacologically active MPA concentration.<sup>2</sup> Therefore, MPAG may indirectly contribute to the overall immunosuppression activity of MPA. Furthermore, MPAG undergoes enterohepatic recirculation (EHR), which generates a secondary peak in the MPA plasma concentration-time profile.<sup>4</sup> This is believed to involve colonic bacterial deconjugation of

---

From the Department of Biomedical and Pharmaceutical Sciences, College of Pharmacy, University of Rhode Island, Kingston. Submitted for publication July 11, 2008; revised version accepted November 5, 2008. Address for correspondence: Sara E. Rosenbaum, PhD, Department of Biomedical and Pharmaceutical Sciences, University of Rhode Island, 41 Lower College Road, Kingston, RI 02881; e-mail: sarar@uri.edu.  
DOI: 10.1177/0091270008329558

the glucuronide metabolite to MPA and subsequent reabsorption of MPA into the systemic circulation. In a recent study in Japanese kidney transplant recipients, the incidence of MPA-related side effects, leucopenia and diarrhea, was 2-fold higher in patients who exhibited EHR than in patients who did not.<sup>5</sup> Repeated direct exposure of the intestinal epithelium to MPA during the EHR process is believed to generate the intestinal toxicity; therefore, better understanding of the EHR is warranted.

Mycophenolic acid acyl glucuronide (AcMPAG) is a minor and pharmacologically active metabolite of MPA.<sup>6</sup> This metabolite often can be quantified in the plasma of patients under therapy with MPA,<sup>7,8</sup> and similar to other acyl glucuronide metabolites, AcMPAG can form adducts with plasma proteins.<sup>7,8</sup> Shipkova et al<sup>8</sup> found a linear relationship between the level of albumin adducts and the AcMPAG AUC. Adduct formation may contribute to MPA-induced toxicity either through direct disruption of protein function or through antigen formation with subsequent hypersensitivity and other immune reactions. Therefore, the ability to predict the extent of exposure to AcMPAG may be useful for the prediction of some MPA-related side effects.

An integrated pharmacokinetic model of MPA and its 2 glucuronidated metabolites would be useful to address the complex interrelationship of EHR between MPA and its metabolites and to provide potentially useful information for MPA pharmacotherapy. The aim of the current analysis was to characterize the pharmacokinetics of MPA, MPAG, and AcMPAG in a group of kidney transplant recipients receiving enteric-coated mycophenolate sodium. This was achieved by (1) developing an integrated pharmacostatistical model to simultaneously describe the MPA, MPAG, and AcMPAG pharmacokinetics and (2) identifying the patient characteristics that can influence the pharmacokinetic parameters.

## METHODS

### Patients and Data Collection

Eighteen stable kidney transplant recipients from the Transplant Services at Rhode Island Hospital entered a study that was aimed to investigate the effects of diabetes mellitus on the pharmacokinetics of MPA and its metabolites.<sup>9</sup> The study protocol was reviewed and approved by the Institutional Review Board at Rhode Island Hospital, and all patients gave informed consent to participate. All patients were

on twice-daily doses (360 or 720 mg every 12 hours) of enteric-coated mycophenolate sodium. For each patient, 13 blood samples were collected at steady-state via an indwelling cannula before dose and at 0.25, 0.5, 0.75, 1.5, 2.0, 3.0, 4.0, 5.0, 7.0, 9.0, 10.0, and 12.0 hours postdose. The blood samples were centrifuged for 10 minutes at 1500 g ambient temperature, and the plasma was stored at  $-70^{\circ}\text{C}$  until analyzed. Serum creatinine, aspartate aminotransferase, alanine aminotransferase, total bilirubin, and serum albumin were monitored on the day of the pharmacokinetic study. Iohexol clearance was used to estimate glomerular filtration rate (GFR) using a validated method for the determination of plasma iohexol.<sup>10</sup> The clinical description of the patients included in the study has been described elsewhere.<sup>9</sup>

### Bioanalytics

Plasma concentrations of MPA, MPAG, and AcMPAG were measured using a previously described high-performance liquid chromatography/ultraviolet (HPLC/UV) method.<sup>11</sup> The assay was linear in the concentration range from 0.2 to 50 mg/L for MPA, 0.5 to 25 mg/L for AcMPAG, and 2 to 500 mg/L for MPAG. The lower limit of quantification for MPA, AcMPAG, and MPAG was 0.2, 0.5, and 2.0 mg/L, respectively.

### Population Pharmacokinetic Analysis

Plasma concentration-time data for MPA, MPAG, and AcMPAG were modeled using a nonlinear mixed-effects approach with NONMEM (Version V, Level 1.1).<sup>12</sup> Double precision and first-order estimation were used.

Pharmacokinetic parameter estimates for MPA, MPAG, and AcMPAG were determined using the following sequential steps. In step 1, single- and multi-compartment pharmacokinetic models with linear elimination were fitted to the MPA concentration-time data to determine the basic pharmacokinetic model. The Akaike information criterion (AIC) was used to discriminate between nonhierarchical models for the selection of a basic pharmacokinetic structural model. In step 2, the pharmacokinetic parameters of the MPA modeling were then used as initial estimates to simultaneously model MPA and MPAG concentrations. The MPAG pharmacokinetics were modeled as a metabolite compartment connected to the central MPA compartment.

A secondary peak in the MPA concentration-time profile, at approximately 6 to 9 hours postdose,

indicative of EHR was observed in 16 of 18 patients. The EHR of MPA through MPAG was modeled in step 3 by presuming a hypothetical gallbladder compartment into which MPAG entered from its central compartment. Based on the time of the secondary peak and the intake of food relative to the dose, the gallbladder compartment was assumed to empty into the depot (gastrointestinal [GI]) compartment at 8 hours. The duration of gallbladder emptying was fixed at 1.5 hours.<sup>13</sup>

In step 4, the AcMPAG pharmacokinetics were modeled as a metabolite compartment connected to the central MPA compartment. Models for AcMPAG pharmacokinetics were developed with the individual parameters of MPA and MPAG fixed to those identified in the final model developed in the third step. Finally, in step 5, a model with an EHR component was included and tested to describe MPA and AcMPAG data as described in step 3. For both metabolites, interconversion between parent and each metabolite was tested.

Unexplained intersubject variability in structural model parameters was estimated using the following model with the random effect  $\eta_j$ :

$$P_j = TV(P)\exp(\eta_j), \quad (1)$$

where  $P_j$  is the individual value for  $P$  in the  $j$ th individual,  $TV(P)$  is the typical value of the pharmacokinetic parameter  $P$  (eg, CL) in the population, and  $\eta_j$  is the difference between both. Residual variability  $\epsilon_{ij,k}$  for the 3 different data sets ( $k = 1, 2, 3$ )—that is, the discrepancy between the individual observed ( $C_{obs,ij}$ )  $i$ th plasma concentration measured in the  $j$ th individual for the respective metabolite and the respective individual model-predicted plasma concentrations ( $C_{pred,ij}$ )—was modeled according to a proportional error model:

$$C_{obs,ij} = C_{pred,ij} \times (1 + \epsilon_{ij,1}) \text{ for MPA.} \quad (2)$$

$$C_{obs,ij} = C_{pred,ij} \times (1 + \epsilon_{ij,2}) \text{ for MPAG.} \quad (3)$$

$$C_{obs,ij} = C_{pred,ij} \times (1 + \epsilon_{ij,3}) \text{ for AcMPAG.} \quad (4)$$

All random effects parameters  $\eta$  and  $\epsilon$  were assumed to be symmetrically distributed with zero mean and variance  $\omega^2$  and  $\sigma^2$ , respectively.

The structural pharmacokinetic model was selected based on model selection criteria (eg, the NONMEM objective function [OFV] and diagnostic plots) and on the ability to predict the individual area under the curve (AUC) calculated by noncompartmental analysis (data not shown). The model-predicted AUC values

were estimated using the individual empirical Bayes (post hoc) pharmacokinetic parameters.

### Covariate Model Building

The standard 3-stage approach<sup>14</sup> was used to evaluate the following patient characteristics as possible covariates for all of the pharmacokinetic parameters of MPA, MPAG, and AcMPAG: age, weight, body surface area, concomitant administration of tacrolimus or cyclosporine, GFR, aspartate aminotransferase, alanine aminotransferase, total bilirubin, serum albumin, diabetes, and ethnicity.

Covariate testing was performed sequentially for MPA, MPAG, and AcMPAG. The influence of continuous covariates (age, weight, body surface area, GFR, aspartate aminotransferase, alanine aminotransferase, total bilirubin, and serum albumin) on the pharmacokinetic parameter  $P$  was modeled according to the following equation:

$$P = TV(P) \times (\text{covariate}/\text{mean covariate})^{\theta_{\text{covariate}}}, \quad (5)$$

where  $TV(P)$  is the typical value of  $P$  for a patient with the mean covariate value, and  $\theta_{\text{covariate}}$  is the estimated effect for the covariate on  $P$ .

It was noted that some parameters were influenced by some continuous covariates (eg, renal function) only when the covariate achieved a critical value. In these cases, the influence of continuous covariates on parameter  $P$  was modeled according to the following equation:

$$P = TV(P_1) \times (\text{covariate}/\text{mean covariate})^{\theta_{\text{covariate}}} \text{ for covariate} \leq \text{cutoff value}, \quad (6)$$

$$P = TV(P_2) \text{ for covariate} > \text{cutoff value}, \quad (7)$$

where  $TV(P_1)$  is the typical value of  $P$  for a patient with the mean covariate value,  $\theta_{\text{covariate}}$  is the estimated effect for the covariate on  $P$  below or equal to the cutoff value, and  $TV(P_2)$  is the typical value of  $P$  for a patient with a covariate value above the cutoff value. The critical values were determined graphically from the plots of the Bayesian post hoc estimates versus covariates.

The influence of categorical covariates (concomitant tacrolimus and cyclosporine, diabetes, and ethnicity) on parameter  $P$  was modeled according to the following equation:

$$P = TV(P) \text{ for the reference covariate value,} \quad (8)$$

$$P = TV(P) \times \theta_{\text{covariate}} \text{ for the investigated covariate value.} \quad (9)$$

In the comparison between hierarchical models, the value of OFV was used in chi-square tests. A change in OFV ( $\Delta$ OFV) of  $>3.84$  (1 degree of freedom) and  $5.99$  (2 degrees of freedom) was initially taken as indicative of a significant change ( $P < .05$ ) when comparing between hierarchical models. If a covariate was statistically significant, it was kept in the model, and a new covariate was added and tested. If not statistically significant, then the covariate was dropped from the model, and the effect of another covariate was evaluated (forward addition). The tentative final model was further tested by eliminating each covariate one at a time to evaluate the  $\Delta$ OFV (backward elimination). The level of significance for reinstating the eliminated covariate into the model was set at  $\Delta$ OFV  $> 10.8$  ( $P < .001$ ).

### Predictive Ability

The predictability of the model was evaluated using the visual predictive check. One hundred data sets were simulated each for MPA, MPAG, and AcMPAG from the final model. The observed data were compared to the 5th, 50th, and 95th percentiles of the simulated data.

## RESULTS

A total of 232 plasma concentrations were obtained for MPA and each of the 2 metabolites (MPAG and AcMPAG) from the 18 kidney transplant recipients. The demographic characteristics of the patients are shown in Table I. The patients were on a triple immunosuppressive therapy, which consisted of prednisone, MPA, and either cyclosporine or tacrolimus.

A 2-compartment model with linear elimination adequately described the MPA data. A 1-compartment model resulted in a higher objective function and worse fit, whereas a 3-compartment model resulted in nonconvergence of the model, possibly due to model overparameterization. The first-order absorption rate constant,  $k_a$  of MPA, was estimated to be  $0.673 \text{ h}^{-1}$ , and this value was fixed during the subsequent modeling of MPAG pharmacokinetics. The inclusion of an absorption lag time was not associated with a better fit of the data.

Disposition of MPAG was initially described using a 1-compartment model with linear elimination. Incorporation of EHR of MPA via MPAG allowed characterization of the secondary peak seen in the MPA plasma concentration profile and led to

a drop in objective function of 34.463, which corresponds to a 26.463-unit decrease in AIC. No interconversion was evident between MPA and MPAG. Thus, a 1-compartment model with linear elimination and EHR of MPA via MPAG was selected as the basic structural pharmacokinetic model for MPA and MPAG.

Graphical analysis of empirical Bayes estimates and univariate analysis were used to identify potential covariates. A significant effect for concomitant medication (tacrolimus or cyclosporine) on  $k_{3G}$ , the rate constant controlling the transfer of MPAG from the central to the gallbladder compartment ( $P < .001$ ), was found. Significant effects for GFR on  $k_{30}$  ( $P < .001$ ) and on  $k_{3G}$  ( $P < .005$ ) were also identified. In the forward addition and backward elimination steps, only the influence of GFR on  $k_{30}$  remained significant ( $P < .001$ ).

Disposition of AcMPAG was initially described using a 1-compartment model with linear elimination. Incorporation of EHR of MPA via AcMPAG led to a drop of 20.281 units in the minimum objective function, and this corresponds to a decrease in 14.281 units in AIC. No interconversion seemed to be evident between MPA and AcMPAG. Thus, a 1-compartment model with linear elimination and EHR of MPA via AcMPAG was selected as the basic structural pharmacokinetic model for MPA and AcMPAG. Graphical analysis of empirical Bayes estimates and univariate analysis identified the following significant covariate effect: GFR on  $FM_{AC}$ , the ratio of the fraction of MPA metabolized to AcMPAG to the volume of distribution of AcMPAG ( $P < .001$ ). In both the forward addition and backward elimination steps, GFR on  $FM_{AC}$  remained significant ( $P < .001$ ).

The final model for MPA and its 2 glucuronidated metabolites, MPAG and AcMPAG, is shown schematically in Figure 1. Table II shows the final population pharmacokinetic parameter estimates. Figure 2 shows the observed and population predicted dose-normalized MPA, MPAG, and AcMPAG time courses. The secondary peak arising from EHR of MPA is well defined. Figure 3 shows the observed versus individual predicted MPA, MPAG, and AcMPAG goodness-of-fit plots.

The predictive ability of the model was evaluated using the visual predictive check. Figure 4 shows the observed data and the lines corresponding to the 5th, 50th, and 95th percentiles of the simulated data ( $n = 100$ ) for MPA, MPAG, and AcMPAG. It can be seen that overall, the final PK model for MPA,

**Table I** Clinical Information of the Kidney Transplant Recipients (n = 18) Studied

Continuous Characteristics	Median	Range (Min-Max)
Age, y	46	18–63
Body weight, kg	85.7	57.0–133
Body surface area, m <sup>2</sup>	2.03	1.59–2.46
Serum creatinine, mg/dL	1.55	1.00–2.70
Serum albumin, g/dL	4.30	3.60–4.80
Aspartate aminotransferase, U/L	18.5	13.0–45.0
Alanine aminotransferase, U/L	18.0	8.0–45.0
Glomerular filtration rate, <sup>a</sup> mL/min/1.73 m <sup>2</sup>	58.0	25.7–100
Dose of mycophenolate sodium, mg/day	720	720–1440
Calcineurin inhibitor dose		
Tacrolimus, mg/d	5.0	4.0–14
Cyclosporine, mg/d	50.0	25.0–125
Prednisone dose, mg/d	5.0	3.8–10.0
Number of samples per patient	13	12–13
Time posttransplant, d	902	187–2744
Categorical Characteristics	Number	%
Gender		
Male	18	100
Concomitant calcineurin inhibitor		
Tacrolimus	10	55.6
Cyclosporine	8	44.4
Concomitant disease		
Diabetic	9	50.0
Nondiabetic	9	50.0
Ethnicity		
Caucasian	10	55.6
African American	5	37.8
Hispanic	3	16.7

a. Estimated using iohexol clearance method and normalized to a body surface area of 1.73 m<sup>2</sup>.

MPAG, and AcMPAG predicts the observed concentrations well. The greatest weakness of the overall model appears to be at  $C_{\max}$  of MPA. This result is not unexpected given the typical variability observed in the peak plasma concentrations from enteric-coated orally administered drugs.

## DISCUSSION

The pharmacokinetics of MPA and its 2 glucuronidated metabolites, MPAG and AcMPAG, were well described by the 6-compartment model that incorporates EHR of MPA via its 2 metabolites, MPAG and AcMPAG. This investigation is the first model-based analysis, which includes the minor but pharmacologically active metabolite AcMPAG and will add to the existing knowledge of MPA disposition in kidney transplant recipients. A population pharmacokinetic

approach was used in the present analysis to estimate the mean pharmacokinetic parameters, quantify interindividual and residual variabilities, and probe the potential influence of certain patient characteristics on the pharmacokinetic parameters. This approach should also help in distinguishing the factors that influence the pharmacokinetics of MPA and each of the 2 metabolites.

The population mean estimate for the MPA absorption rate constant,  $k_a$  of 0.67 h<sup>-1</sup> in our study, is lower than the reported literature values of 2.27 to 4.10 h<sup>-1</sup>.<sup>15,16</sup> This difference is attributed to the formulation of MPA (ie, enteric-coated mycophenolate sodium in this study vs non-enteric-coated mycophenolate mofetil in the other studies). Population mean estimates for MPA apparent clearance and volumes of distribution for the central compartment were similar to the literature values of 11.9 to 33.0 L/h<sup>15-19</sup> and

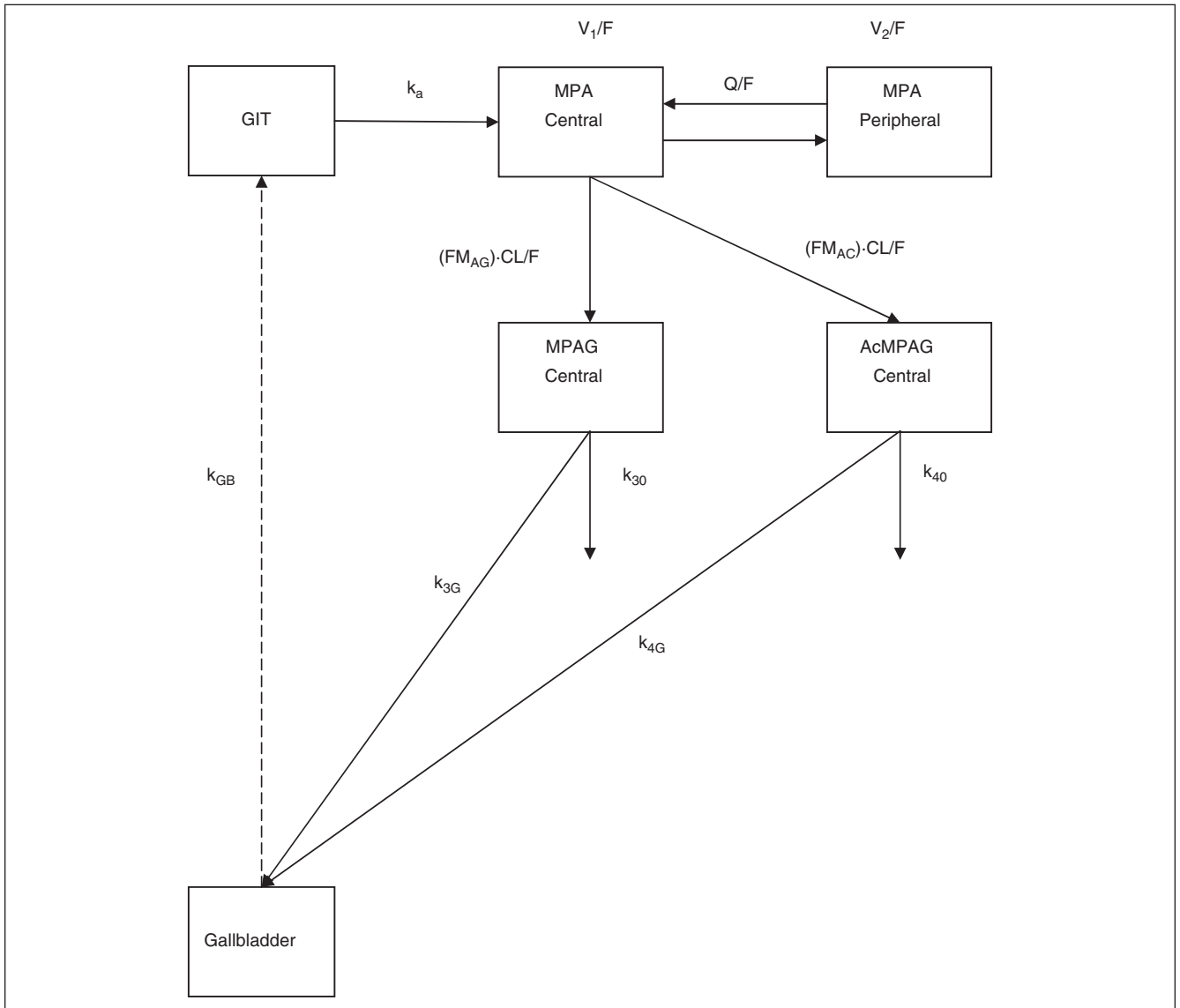


Figure 1. Population pharmacokinetic model of mycophenolic acid (MPA), mycophenolic glucuronide (MPAG), and mycophenolic acyl glucuronide (AcMPAG) containing enterohepatic recirculation (EHR) that comprises 6 compartments: GIT, gastrointestinal tract, MPA central, MPA peripheral, MPAG central, AcMPAG central, and gallbladder.  $CL/F$  and  $Q/F$  are apparent clearance of MPA and apparent intercompartmental clearance.  $V_1/F$  and  $V_2/F$  are the apparent volumes of distribution of MPA in central and peripheral compartments, respectively.  $FM_{AG}$  and  $FM_{AC}$  are the fractions of MPA metabolized to MPAG and AcMPAG, respectively, normalized by their volume of distributions. First-order rate constants are as follows:  $k_a$ , absorption of MPA;  $k_{30}$ , overall elimination for MPAG;  $k_{40}$ , overall elimination for AcMPAG;  $k_{3G}$ , rate constant for the transfer of MPAG from the central to the gallbladder compartment;  $k_{4G}$ , rate constant for the transfer of AcMPAG to the gallbladder compartment;  $k_{GB}$ , rate constant for the release of recirculated MPA from MPAG and AcMPAG into the depot compartment.

10.3 to 97.7 L,<sup>15,16,18,19</sup> respectively. The population mean estimated  $k_a$  of MPA in this study was approximately 1.5-fold greater than the elimination constant ( $k_{10} = 0.409 \text{ h}^{-1}$ ), calculated from the ratio of  $CL/F$  and  $V_1/F$  from the central compartment, suggesting that

the elimination of MPA through both bile and urine is slower than absorption in the gastrointestinal tract.

EHR of MPA via its 2 glucuronidated metabolites was successfully modeled using a model that incorporated the effect of gallbladder emptying. This

**Table II** Parameter Estimates of Final Population Pharmacokinetic Model for MPA, MPAG, and AcMPAG in Kidney Transplant Recipients

Parameter	Estimate (%RSE)	% Interindividual Variability (%RSE)	% Intraindividual Variability (%RSE)
MPA			69.9 (15.3)
$k_a$ , h <sup>-1</sup>	0.673 (24.8)		
CL/F, L/h	10.6 (11.1)	21.4 (66.1)	
$V_1$ /F, L	25.9 (34.9)	87.8 (32.0)	
Q/F, L/h	8.11 (24.2)		
$V_2$ /F, L	39.6 (86.9)	239 (248)	
MPAG			19.4 (32.1)
$FM_{AC}$ , L <sup>-1</sup>	0.385 (27.3)	34.6 (85.8)	
$k_{30}$ , h <sup>-1</sup> ; GFR ≤80 mL/min/1.73 m <sup>2</sup>			
$k_{30} = a \times (GFR/51.6)^b$			
a	0.175 (34.7)	29.1 (199)	
b	0.335 (262)		
$k_{30}$ , h <sup>-1</sup> ; GFR >80 mL/min/1.73 m <sup>2</sup>	0.323 (28.4)	29.1 (199)	
$k_{3G}$ , h <sup>-1</sup>	0.154 (28.8)		
$k_{CB}$ , h <sup>-1</sup>	0.00725 (167)	35.9 (260)	
AcMPAG			17.8 (23.2)
$FM_{AC}$ , L <sup>-1</sup> ; GFR ≤60 mL/min/1.73 m <sup>2</sup>			
$FM_{AC} = c (GFR/45.3)^d$			
c	0.0138 (17.5)	24.6 (68.7)	
d	-1.95 (11.7)		
$FM_{AC}$ , L <sup>-1</sup> ; GFR >60 mL/min/1.73 m <sup>2</sup>	0.0132 (15.1)	24.6 (68.7)	
$k_{40}$ , h <sup>-1</sup>	0.206 (13.8)	48.8 (47.1)	
$k_{4G}$ , h <sup>-1</sup>	0.146 (26.5)	67.3 (41.1)	

% RSE, percent relative standard error (SE/estimate multiplied by 100%); MPA, mycophenolic acid;  $k_a$ , absorption rate constant; CL/F, apparent clearance;  $V_1$ /F, apparent volume of central compartment; Q/F, intercompartmental clearance;  $V_2$ /F, apparent volume of peripheral compartment; MPAG, mycophenolic glucuronide;  $FM_{AC}$ , ratio of the fraction of MPA metabolized to MPAG to the volume of distribution of MPAG;  $k_{30}$ , elimination rate constant of MPAG; GFR, glomerular filtration rate;  $k_{3G}$ , rate constant for the transfer of MPAG from the central to the gallbladder compartment;  $k_{CB}$ , rate constant for the release of recirculated MPA from MPAG and AcMPAG into the depot compartment; AcMPAG, mycophenolic acyl glucuronide;  $FM_{AC}$ , ratio of the fraction of MPA metabolized to AcMPAG to volume of distribution of AcMPAG;  $k_{40}$ , elimination rate constant of AcMPAG;  $k_{4G}$ , rate constant for the transfer of AcMPAG from the central to the gallbladder compartment.

model is distinct from the EHR pharmacokinetic model developed for MPA by Funaki,<sup>20</sup> which only incorporated MPA during EHR. In contrast to the integrated MPA and MPAG pharmacokinetic model developed by Cremers et al<sup>19</sup> that incorporated an enterohepatic cycle, the present model assumed that the release of bile from the gallbladder occurred in short bursts at a constant rate over 1.5 hours and that the release of the glucuronide metabolites occurred as a first-order process during the 1.5-hour period. In addition, in the present model, the metabolic clearance of MPA included conversion to both MPAG and AcMPAG. Moreover, the performance of these 2 published models is difficult to evaluate because their predictive performance was not reported. Thus, the authors believe that the current EHR model of MPA, evaluated using the predictive visual check, represents the most comprehensive and physiological model of the EHR of MPA to date.

It must be noted that owing to the limited number of patients included and the large number of parameters associated with the model, the estimates of  $V_2$ /F and  $k_{CB}$  were associated with a large degree of uncertainty. The main weakness of the present model is the poor estimation and very low value of  $k_{CB}$ . Two of the patients in the study did not display secondary peaks corresponding to EHR. Additional variability may arise from concurrent medication; half the patients in the study were taking concurrent cyclosporine and the other half concurrent tacrolimus. Cyclosporine is a known inhibitor of the efflux transporter multidrug resistance protein 2 (MRP2),<sup>21</sup> and thus it is possible that EHR was inhibited in these patients. Although we were unable to identify concurrent tacrolimus or cyclosporine as significant covariates, it is likely that the study did not have sufficient power to differentiate between the 2 groups. We are presently collecting

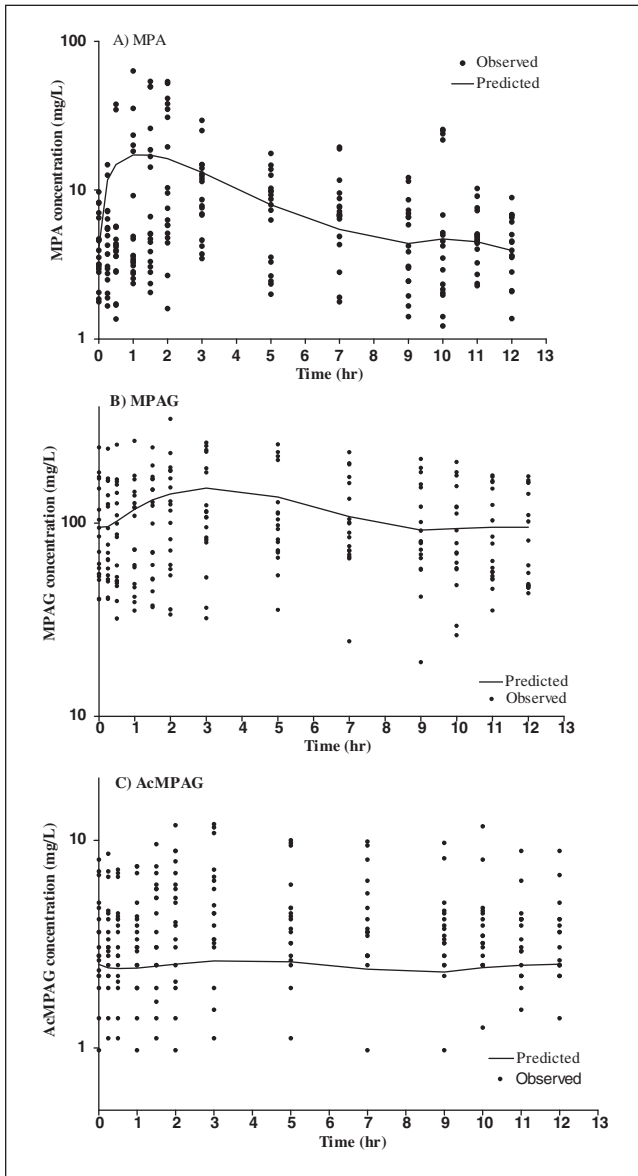


Figure 2. Semilog dose-normalized observed (dot) and population-predicted (solid line) (A) mycophenolic acid (MPA), (B) mycophenolic glucuronide (MPAG), and (C) mycophenolic acyl glucuronide (AcMPAG) plasma concentration versus time profiles.

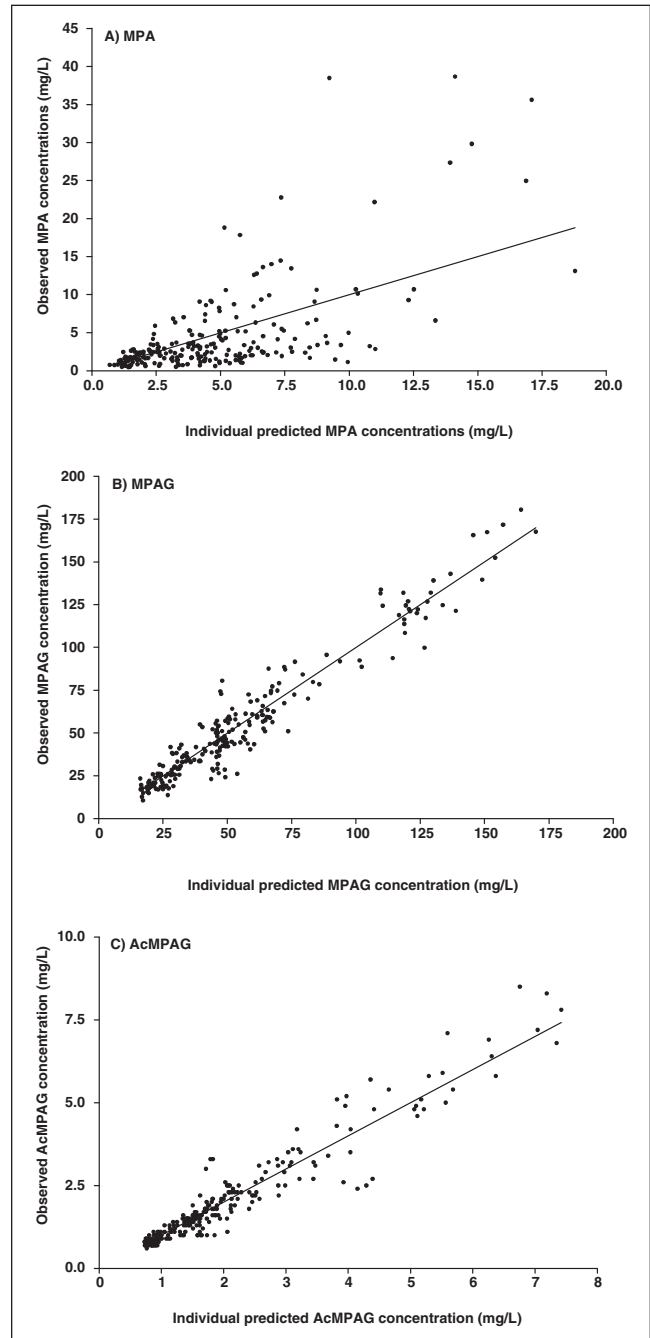


Figure 3. (A) Mycophenolic acid (MPA), (B) mycophenolic glucuronide (MPAG), and (C) mycophenolic acyl glucuronide (AcMPAG) observed versus individual predicted concentrations (solid line is the line of identity).

data that will allow us to more precisely estimate  $k_{GB}$  and identify factors that influence EHR.

Based on the ratio of  $k_{3G}$  and  $k_3$  ( $k_{30} + k_{3G}$ ), the percentage of MPAG excreted in the bile is estimated to be approximately 32% at GFR >80 mL/min/1.73 m<sup>2</sup> and increases to approximately 49% at GFR of 40 mL/min/1.73 m<sup>2</sup>. Thus, the model predicts an increase in biliary excretion of MPAG during renal

impairment. This finding is supported by results from animal studies that the biliary excretion of MPAG was significantly increased when MPA was administered

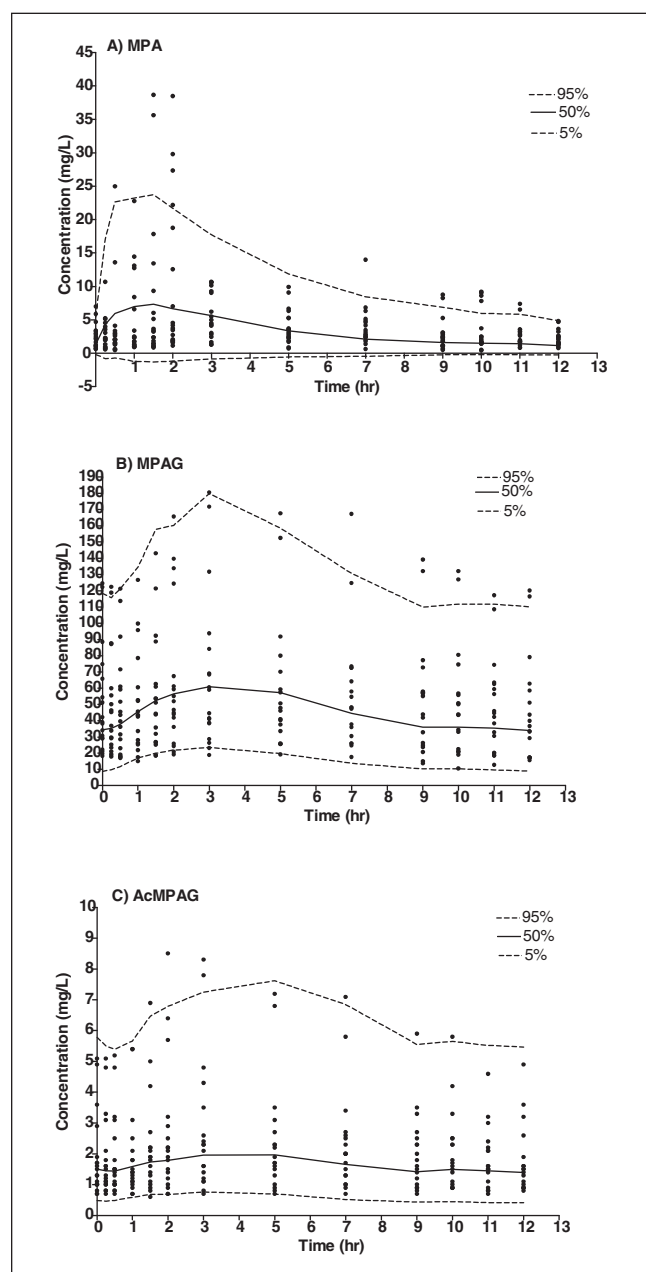


Figure 4. Visual predictive check. Observed data compared to the 95th, 50th, and 5th percentiles of the simulated (100) data sets.

intravenously to rats with acute renal failure.<sup>22</sup> The implication of this finding is that more MPAG will be subjected to EHR during renal dysfunction, leading to higher concentrations of the parent MPA in the intestine and potentially greater incidence of gastrointestinal toxicity.

A new finding of this study is that the model suggests that AcMPAG may also undergo EHR. Thus, AcMPAG excreted to the gastrointestinal tract via bile could serve as a secondary source for MPA absorption via deglucuronidation. However, this hypothesis cannot be confirmed by modeling alone and needs further characterization through pharmacokinetic studies in animal models.

Covariate modeling identified GFR, measured precisely using the iohexol clearance method, as a significant covariate on the elimination rate constant of MPAG ( $k_{30}$ ) and  $FM_{AC}$  of AcMPAG. Renal dysfunction was found to explain 22.6% of the interindividual variability in MPAG's elimination rate constant. A 50% decrease in GFR from GFR of 80 mL/min/1.73 m<sup>2</sup> would result in a 50.3% decrease in the elimination rate of MPAG. This finding itself was not unexpected because MPAG is mainly eliminated by renal excretion, with the involvement of active tubular secretion, since its apparent renal clearance was found to exceed creatinine clearance.<sup>4</sup> The carrier system responsible for this transport could be the organic anion transporter located in the basolateral membrane of cells in the proximal tubule of the kidneys. Wolff et al<sup>23</sup> reported that MPA, MPAG, and AcMPAG potentially interact with human organic anion transporters 1 (hOAT1) and 3 (hOAT3) in the kidney and thereby may interfere with the renal secretion of antiviral drugs, cortisol, and other organic anions. With the development of renal failure and the subsequent accumulation of the waste normally eliminated by the kidneys (uremic toxins), renal secretion of organic ions is decreased by the direct inhibition of the renal transport of organic anion transporters. Organic anion transporters' expression levels had also been found to decrease in patients with renal disease.<sup>24</sup> These factors may explain the decrease in MPAG elimination during renal dysfunction.

Renal function was found to be a predictor for the  $FM_{AC}$  of AcMPAG and explained 26.4% of its interindividual variability. A 50% decrease in GFR from GFR of 60 mL/min/1.73 m<sup>2</sup> would result in a 134% increase in the  $FM_{AC}$  of AcMPAG, suggesting that the fraction of MPA metabolized to AcMPAG was increased by the same amount, assuming no change in the volume of distribution of AcMPAG. This may explain higher AcMPAG concentrations observed in patients with renal dysfunction, which may be due to an increase in the amount of MPA available for glucuronidation to AcMPAG during renal dysfunction. As discussed previously, this

finding is consistent with a study in rats, which found the biliary excretion of MPAG to be increased in rats with renal failure.<sup>22</sup> Thus, more MPAG would be available for deglucuronidation to MPA in the gastrointestinal tract. Also, it has been found that free MPA concentrations and the free fraction of MPA are elevated in patients with severe renal failure when on chronic MPA therapy.<sup>17</sup> This appears to be due to the uremic state and by competition for albumin binding sites with the renally eliminated metabolite MPAG. Therefore, both these 2 factors will result in the increased fraction of MPA metabolized to AcMPAG during renal dysfunction. It must be noted that this study was performed on only 18 patients. Thus, the other patient characteristics tested (age, weight, body surface area, concomitant tacrolimus or cyclosporine, liver function tests, serum albumin, diabetes, and ethnicity) revealed to be statistically nonsignificant on the pharmacokinetic parameters of MPA, MPAG, and AcMPAG should be reevaluated in a larger, more diverse patient population.

Because of substantial interindividual variability in MPA pharmacokinetics, therapeutic drug monitoring of MPA seems to be necessary to minimize toxicity and to ensure adequate MPA exposure to prevent transplant rejection. Several studies have demonstrated a relationship between plasma MPA AUC and clinical outcomes.<sup>25,26</sup> Low AUC of total MPA has been associated with a higher incidence of acute organ rejection in heart and kidney transplant recipients. Thus, a population model for MPA and its metabolites could be used as an aid in therapeutic drug monitoring of MPA to compute individual mean estimates of the AUCs of MPA, MPAG, and AcMPAG. The exploratory population model presented in this study constitutes an important first step in the development of a clinically useful model. Further studies with additional patients are warranted to further probe this model and to investigate the influence of patient characteristics.

In conclusion, a 6-compartment model has been established for the pharmacokinetics of MPA and its 2 glucuronidated metabolites. Renal dysfunction was found to influence the pharmacokinetic parameters of MPAG and AcMPAG. The model provides a first step in the development of a clinically useful model to prospectively individualize MPA therapy to achieve a target systemic exposure of either parent compound, its 2 glucuronidated metabolites, or both. In addition, the model may help to further

elucidate the manner in which MPA and its 2 glucuronidated metabolites contribute to the overall clinical effects of MPA therapy, including immunosuppression and gastrointestinal side effects.

Financial disclosure: None declared.

## REFERENCES

1. Mele TS, Halloran PF. The use of mycophenolate mofetil in transplant recipients. *Immunopharmacology*. 2000;47:215-245.
2. Nowak I, Shaw LM. Mycophenolic acid binding to human serum albumin: characterization and relation to pharmacodynamics. *Clin Chem*. 1995;41:1011-1017.
3. Mackenzie PI. Identification of uridine diphosphate glucuronosyltransferases involved in the metabolism and clearance of mycophenolic acid. *Ther Drug Monit*. 2000;2000:10-13.
4. Bullingham RE, Nicholls AJ, Kamm BR. Clinical pharmacokinetics of mycophenolate mofetil. *Clin Pharmacokinet*. 1998;34: 429-455.
5. Sugioka N, Sasaki T, Kokuhu T, et al. Clinical pharmacokinetics of mycophenolate mofetil in Japanese renal transplant recipients: a retrospective cohort study in a single center. *Biol Pharm Bull*. 2006;29:2099-2105.
6. Tedesco-Silva H, Bastien MC, Choi L, et al. Mycophenolic acid metabolite profile in renal transplant patients receiving enteric-coated mycophenolate sodium or mycophenolate mofetil. *Transplant Proc*. 2005;37:852-855.
7. Shipkova M, Armstrong VW, Wieland E, et al. Identification of glucoside and carboxyl-linked glucuronide conjugates of mycophenolic acid in plasma of transplant recipients treated with mycophenolate mofetil. *Br J Pharmacol*. 1999;126:1075-1082.
8. Shipkova M, Armstrong VW, Weber L, et al. Pharmacokinetics and protein adduct formation of the pharmacologically active acyl glucuronide metabolite of mycophenolic acid in pediatric renal transplant recipients. *Ther Drug Monit*. 2002;24:390-399.
9. Patel CG, Richman K, Yang D, Yan B, Gohh RY, Akhlaghi F. Effect of diabetes mellitus on mycophenolate sodium pharmacokinetics and inosine monophosphate dehydrogenase activity in stable kidney transplant recipients. *Ther Drug Monit*. 2007;29: 735-742.
10. Soman RS, Zahir H, Akhlagh IF. Development and validation of an HPLC-UV method for determination of iohexol in human plasma. *J Chromatogr B*. 2005;816:339-343.
11. Patel CG, Akhlaghi F. High-performance liquid chromatography method for the determination of mycophenolic acid and its acyl and phenol glucuronide metabolites in human plasma. *Ther Drug Monit*. 2006;28:116-122.
12. Beal SL, Sheiner LB. *NONMEM Users Guide*. San Francisco: NONMEM Project Group, University of California, San Francisco; 1992.
13. Hofmann AF, Molino G, Milanese M, Belforte G. Description and simulation of a physiological pharmacokinetic model for the metabolism and enterohepatic circulation of bile acids in man: cholic acid in healthy man. *J Clin Invest*. 1983;71:1003-1022.
14. Mandema JW, Verotta D, Sheiner LB. Building population pharmacokinetic-pharmacodynamic models: I. Models for covariate effects. *J Pharmacokinet Biopharm*. 1992;20:511-528.

15. Shum B, Duffull SB, Taylor PJ, Tett SE. Population pharmacokinetic analysis of mycophenolic acid in renal transplant recipients following oral administration of mycophenolate mofetil. *Br J Clin Pharmacol*. 2003;56:188-197.
16. van Hest RM, van Gelder T, Vulto AG, Mathot RAA. Population pharmacokinetics of mycophenolic acid in renal transplant recipients. *Clin Pharmacokinet*. 2005;44:1083-1096.
17. Johnson HJ, Swan SK, Heim-Duthov KL, Nicholls AJ, Tsina I, Tarnowski T. The pharmacokinetics of a single oral dose of mycophenolate mofetil in patients with varying degrees of renal function. *Clin Pharmacol Ther*. 1998;63:512-518.
18. van Hest RM, Mathot RAA, Pescovitz MD, Gordon R, Mamelok RD, van Gelder T. Explaining variability in mycophenolic acid exposure to optimize mycophenolate mofetil dosing: a population pharmacokinetic meta-analysis of mycophenolic acid in renal transplant recipients. *J Am Soc Nephrol*. 2006;17:871-880.
19. Cremers S, Schoemaker R, Scholten E, et al. Characterizing the role of enterohepatic recycling in the interactions between mycophenolate mofetil and calcineurin inhibitors in renal transplant patients by pharmacokinetic modelling. *Br J Clin Pharmacol*. 2005;60:249-256.
20. Funaki T. Enterohepatic circulation model for population pharmacokinetic analysis. *J Pharm Pharmacol*. 1999;10:1143-1148.
21. Westley IS, Brogan LR, Morris RG, Evans AM, Sallustio BC. Role of MRP2 in the hepatic disposition of mycophenolic acid and its glucuronide metabolites: effect of cyclosporine. *Drug Metab Dispos*. 2006;34:261-266.
22. Saitoh H, Kobayashi M, Oda M, Nakasato K, Kobayashi M, Tadano K. Characterization of intestinal absorption and enterohepatic circulation of mycophenolic acid and its 7-O-glucuronide in rats. *Drug Metab Pharmacokinet*. 2006;21:406-413.
23. Wolff NA, Burckhardt BC, Burckhardt G, Oellerich M, Armstrong VW. Mycophenolic acid (MPA) and its glucuronide metabolites interact with transport systems responsible for excretion of organic anions in the basolateral membrane of the human kidney. *Nephrol Dial Transplant*. 2007;22:2497-2503.
24. Sakurai Y, Motohashi H, Ueo H, et al. Expression levels of renal organic anion transporters (OATs) and their correlation with anionic drug excretion in patients with renal diseases. *Pharm Res*. 2004;21:61-67.
25. Shaw LM, Korecka M, DeNofrio D, Brayman KL. Pharmacokinetic, pharmacodynamic, and outcome investigations as the basis for mycophenolic acid therapeutic drug monitoring in renal and heart transplant patients. *Clin Biochem*. 2001;34:17-22.
26. Pillans PI, Rigby RJ, Kubler P, et al. A retrospective analysis of mycophenolic acid and cyclosporin concentrations with acute rejection in renal transplant recipients. *Clin Biochem*. 2001;34:77-81.